AIP | Applied Physics Letters

Magnetoelectric coupling of multiferroic chromium doped barium titanate thin film probed by magneto-impedance spectroscopy

Jyoti Shah and Ravinder K. Kotnala

Citation: Applied Physics Letters **104**, 142901 (2014); doi: 10.1063/1.4870263
View online: http://dx.doi.org/10.1063/1.4870263
View Table of Contents: http://scitation.aip.org/content/aip/journal/apl/104/14?ver=pdfcov
Published by the AIP Publishing

Magnetoelectric coupling of multiferroic chromium doped barium titanate thin film probed by magneto-impedance spectroscopy

Jyoti Shah[a] and Ravinder K. Kotnala[b]
Multiferroic and Magnetics Laboratory, CSIR-National Physical Laboratory, Dr. K.S. Krishnan Road, New Delhi 110012, India

(Received 28 February 2014; accepted 18 March 2014; published online 7 April 2014)

Thin film of $BaTiO_3$ doped with 0.1 at. % Cr (Cr:BTO) has been prepared by pulsed laser deposition technique. Film was deposited on $Pt/SrTiO_3$ substrate at 500 °C in 50 mTorr Oxygen gas pressure using KrF (298 nm) laser. Polycrystalline growth of single phase Cr:BTO thin film has been confirmed by grazing angle X-ray diffraction. Cr:BTO film exhibited remnant polarization 6.4 $\mu C/cm^2$ and 0.79 MV/cm coercivity. Magnetization measurement of Cr:BTO film showed magnetic moment 12 emu/cc. Formation of weakly magnetic domains has been captured by magnetic force microscopy. Theoretical impedance equation fitted to experimental data in Cole-Cole plot for thin film in presence of transverse magnetic field resolved the increase in grain capacitance from 4.58×10^{-12} to 5.4×10^{-11} F. Film exhibited high value 137 mV/cm-Oe magneto-electric (ME) coupling coefficient at room temperature. The high value of ME coupling obtained can reduce the typical processing steps involved in multilayer deposition to obtain multiferrocity in thin film. Barium titanate being best ferroelectric material has been tailored to be multiferroic by non ferromagnetic element, Cr, doping in thin film form opens an avenue for more stable and reliable spintronic material for low power magnetoelectric random excess memory applications. © *2014 AIP Publishing LLC*. [http://dx.doi.org/10.1063/1.4870263]

Multiferroic thin films are technologically important in spintronic devices due to low power consumption.[1,2] Room temperature multiferrocity has been intensively investigated in laminates and bilayer thin films.[3–7] It has been observed that magnetoelectric (ME) coupling in laminates arises due to magnetostriction and piezoelectricity.[8,9] Investigation on origin of magnetoelectric coupling in bilayer and epitaxial films has been also reported.[10–12] The combined effect of Maxwell-Wagner effect and magnetoresistance resulted in to magnetodielectric response in manganites $RMnO_3$.[13,14] Deconvolution of intrinsic film and extrinsic Maxwell-Wagner relaxation in $BiMnO_3$ and $BiFeO_3$ films were attained by fitting frequency dependent data to an adequate equivalent circuit model.[15] In single crystal $LuFe_2O_4$, origin of magnetoelectric effect by interfacial effect was ruled out by impedance spectroscopy.[16] In this work, single phase Cr:BTO thin film has been investigated for magnetoelectric coupling at room temperature. We have earlier reported room temperature magnetoelectric coupling in bulk Cr-doped BTO.[17] The role of individual capacitance and resistance of grains, grain boundaries, and electrode by applying magnetic field has been investigated by theoretical impedance equation fitted to experimental data in Cole-Cole plot. Further magnetoelectric coupling was confirmed by dynamic mode measurement using lock-in amplifier.

Target of 0.1 at. % Cr:BTO for thin film deposition was synthesized by chemical method. The synthesis process has been reported in our earlier work.[17] For preparing target, annealed powder was pressed into 1 inch diameter circular pellet for target and kept at 1300 °C for 10 h for its densification. Thin film was deposited by Pulsed Laser Deposition (PLD) onto $Pt/SrTiO_3$ (Pt/STO) (100) substrate at temperature 500 °C in Oxygen gas pressure 50 mTorr inside the Vacuum System (Excel Instruments, India). The energy density ~2.5 J/cm^2 of pulsed laser was used. After deposition, thin film was annealed *in-situ* at 700 °C for 1 h. Top circular Pt electrodes of 1 mm diameter were deposited on the film by RF-sputtering. Crystalline phase of thin film was analyzed by grazing angle incidence X-ray diffraction using Philips X'Pert-PRO (Pan-Analytic). Polarization vs. electric field plot of Cr:BTO film was taken by thin film P-E loop tracer (Marine India). Magnetization measurement of film was carried out by Vibrating Sample Magnetometers (VSM, Lake Shore, USA). Thin film topography and magnetic domain pattern were captured by Atomic/Magnetic Force Microscopy (AFM/MFM) using Veeco nanoscope-5 in tapping mode. Capacitance and impedance plot of thin were measured by Wayne-Kerr impedance analyzer 6500B (UK). Magnetoelectric coupling coefficient of Cr:BTO thin film was determined by in-house built setup in dynamic mode using lock-in amplifier (Sigma), power amplifier, Helmholtz coil, AC/DC Hall probe (FW-Bell), and 10 in. pole diameter electromagnet with highly homogeneous DC magnetic field.

Crystalline nature of deposited Cr:BTO thin film has been analysed by X-ray diffraction pattern as shown in Figure 1(a). It confirms polycrystalline growth of Cr:BTO film. Cr:BTO planes identified as (111), (002), (200), and (220) of pure barium titanate tetragonal structure along with platinum peaks presence.

Ferroelectric nature of Cr:BTO thin film has been determined by polarization vs. electric field (PE) loop shown in Figure 1(b). The PE loop confirmed that Cr:BTO film was ferroelectric in nature. Maximum polarization of film was 23 $\mu C/cm^2$ with remnant polarization 6.4 $\mu C/cm^2$ and

[a]E-mail: shah.jyoti1@gmail.com
[b]Author to whom correspondence should be addressed. Electronic addresses: rkkotnala@nplindia.org and rkkotnala@gmail.com. Tel.: 91-11-45608599. Fax: 91-11-45609310.

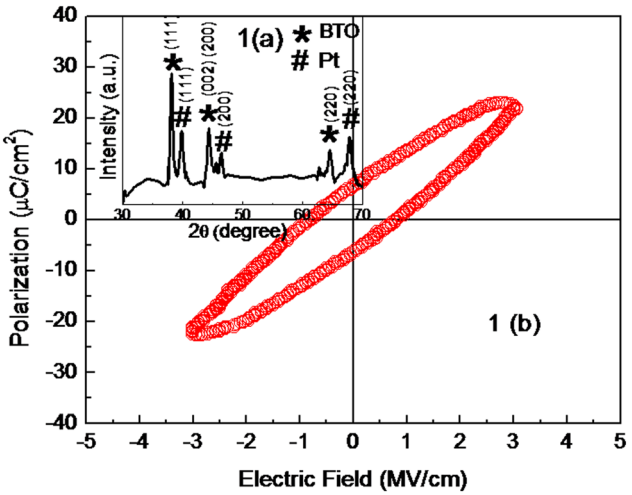

FIG. 1. (a) Grazing angle incident X-ray diffraction pattern of Cr:BTO thin film. (b) Polarization vs. electric field plot at 50 Hz for thin film.

coercive field of 0.79 MV/cm. The remnant polarization value of polycrystalline Cr:BTO film is lower than the reported Mn and Fe doped BTO film deposited on STO substrate by PLD.[18,19] The large value of coercivity reveals dead layer formation by defects/dislocations at grain boundaries.

Induction of magnetism in BTO by transition element has been widely reported in literature.[20–23] Magnetization (M-H) of Cr:BTO thin film has been determined by VSM as shown in Figure 2(a). Magnetic signal observed by Cr:BTO film was obtained by subtracting it from Pt/STO substrate signal. The unsaturated magnetic moment value of 12 emu/cc has been recorded at 5 kOe. Saturation of magnetic moment in 20% Fe:BTO film has been reported at 20 kOe.[24] It may be quite possible that exchange interaction among magnetic ions is not strongly long range ordered due to less concentration of Cr in BTO which leads to high field saturation condition. Ferromagnetism in Mn-doped BTO thin film has been interpreted on the basis of bound magnetic polarons formation by oxygen vacancy.[18] Recently, transformation of antiferromagnetism to ferromagnetism in $Eu_{0.5}Ba_{0.5}TiO_{3-\delta}$ thin film due to oxygen vacancies has been reported.[25] Ferromagnetism in 0.1 at. % Cr:BTO induced due to Cr^{3+} ion incorporation at Ti^{4+} site in BTO lattice will produce oxygen vacancy that leads to long range exchange interaction among Cr^{3+} ions. The lower value of remnant electric polarization also confirms the presence of interfacial defects in the film.

Surface morphology and magnetic domains of thin film have been studied by taking AFM image on 15 μm scan length, 57.4 nm height, and MFM image of the same scan length by vertical phase sweep of 1.5° are shown in Figures 2(b) and 2(c). A smooth platform of uniform color of film reveals smooth growth of thin film. A few large particulates and microcracks are visible as pink and dark brown colors exhibiting high and low atomic force exerted on AFM tip. Particulate formation on thin film by PLD has been explained due to laser energy density and target material.[26,27] Formation of domain pattern with labyrinthine stripes in Co/Pd film has been also captured on a 10 μm length scale by others.[28] The magnetic domains recorded in the MFM image are clearly visible in the form of alternating dark and bright contrast fringes, exhibiting strong and weak magnetic force on MFM tip. The size of the domain in this is about 1–2 μm in width. Similar bigger 4–5 μm ferromagnetic domains have been reported in V/Cr doped TiO_2 thin films.[29] MFM images qualitatively further supports the quantitative magnetization of film obtained by MH loop.

Impedance spectroscopy of Cr:BTO has been performed with zero magnetic field and in presence of 5000 G magnetic field as shown in Figure 3. Cole-Cole plot of Cr:BTO film yielded single semicircle. According to brick model, grains and grain boundaries exhibited identical ideal microstructure formed by separated arcs. Contrary to brick model variations in grain size and grain boundary conductivities in real materials lead to depression of the boundary arc.[30] In order to distinguish relaxation frequencies of depressed arcs corresponding to grains and grain boundaries, curve of Z′ vs. Z″/f has been plotted[31,32] as shown in Figure 4. The individual contribution of relaxation frequency of grain f_g, grain boundary f_{gb}, and electrode f_{el} has been extracted by fitting

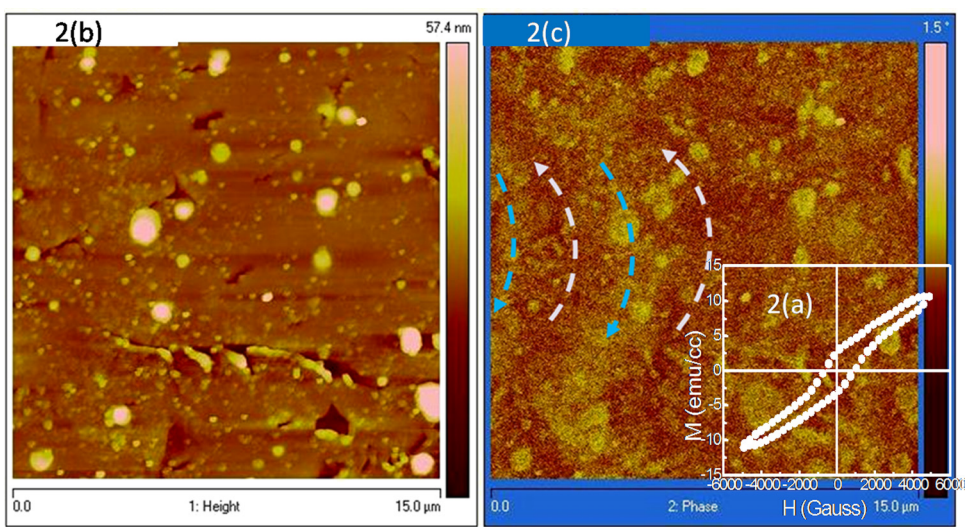

FIG. 2. (a) M (magnetic moment) vs. H (magnetic field) loop for Cr:BTO thin film. (b) Room temperature AFM image and (c) the corresponding MFM image of the Cr:BTO film taken on the scale of 15 μm.

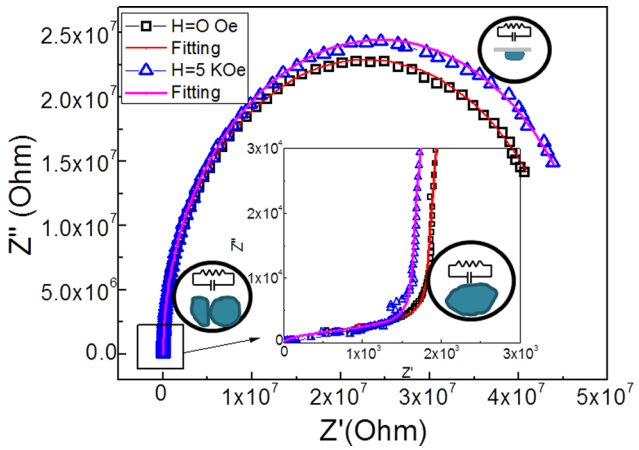

FIG. 3. Impedance spectroscopy plot Z″ vs. Z′ at zero and 5 kOe magnetic field and theoretical plot fitting to experimentally observed curves and corresponding frequency response of grain, grain boundary, and electrode as RC combination, inset shows close view fitting of theoretical plot on two curves.

theoretical impedance equation to experimental Cole-Cole plot. The following impedance equations have been used to plot:[33]

$$Z' = \frac{R_g}{1+\left(\frac{f}{f_g}\right)^2} + \frac{R_{gb}}{1+\left(\frac{f}{f_{gb}}\right)^2} + \frac{R_{el}}{1+\left(\frac{f}{f_{el}}\right)^2}, \quad (1)$$

$$Z'' = \frac{R_g\left(\frac{f}{f_g}\right)}{1+\left(\frac{f}{f_g}\right)^2} + \frac{R_{gb}\left(\frac{f}{f_{gb}}\right)}{1+\left(\frac{f}{f_{gb}}\right)^2} + \frac{R_{el}\left(\frac{f}{f_{el}}\right)}{1+\left(\frac{f}{f_{el}}\right)^2}, \quad (2)$$

where R_g, R_{gb}, R_{el} and f are grain, grain boundary, electrode resistances and experimental frequency sweep respectively.

Since the grain relaxation frequency is at least two order higher than grain boundary relaxation frequency $f_g \gg f_{gb} \gg f_{el}$, then

$$Z' \approx \frac{R_g}{1+\left(\frac{f}{f_g}\right)^2}, \quad (3)$$

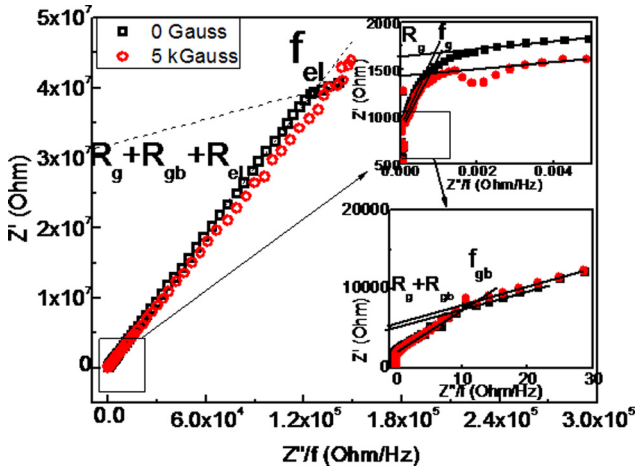

FIG. 4. Z′ (Ohm) vs. Z″/f (Ohm/Hz) curve in absence and presence of 5 kOe magnetic field showing slopes and intercepts inset showing zoomed image of high frequency plots.

$$Z'' \approx \frac{R_g\left(\frac{f}{f_g}\right)}{1+\left(\frac{f}{f_g}\right)^2}. \quad (4)$$

It may be written as

$$Z' \approx f_g(Z''/f), \quad (5)$$

where f_g grain relaxation frequency is the slope of Z′ vs Z″/f plot. Similarly, relaxation frequencies of grain boundary and electrodes can be obtained by slopes of plot and intercepts as grain and grain boundary resistances using relations

$$Z' \approx R_g + f_{gb}(Z''/f), \quad (6)$$

$$Z' \approx R_g + R_{gb} + f_{el}(Z''/f). \quad (7)$$

Values of resistances and frequencies taken by the slope and intercept from Z′ vs Z″/f plot putted in Eqs. (1) and (2). Such obtained values of resistances and relaxation frequencies provided initial theoretical curve fitting to the experimental Cole-Cole plot. However, theoretical curve obtained from Eqs. (1) and (2) was not perfectly fit with to the experimental plot since there was the possibility of error by taking manual values of slopes. Further, perfect fitting was obtained by varying the resistances and frequency values. Theoretical equations were perfectly fitted for high frequency arcs also. The change in resistances of grain, grain boundaries, and electrodes determined from fitting equations after applied magnetic field are shown in Table I. Chromium doping in BTO has induced the magnetism as observed by M-H loop and magnetic domain formation in MFM image. It has been observed by curve fitting that grains exhibit more resistance 1830 Ω than grain boundaries resistance 300 Ω. According to Maxwell-Wagner (M-W) capacitor model, at low frequency charge carrier at low resistive layer, grain boundary, will respond and most of the voltage would drop across highly resistive grains or at electrode interface. This would increase the apparent capacitance of the film. However, in this case grain boundary capacitance and electrode interface capacitance have not been increased inspite of higher resistance compared to grains by applying magnetic field (Table I). Grain boundary capacitance value obtained has been three times 1.3×10^{-9} F higher than grain capacitance

TABLE I. Deconvoluted capacitances, resistances, and time constant of grain, grain boundary, and electrodes by theoretical fitting curves without and with 5 kOe magnetic field.

Cr:BTO	0 G	5 kG
R_g	1830 Ω	1634 Ω
R_{gb}	300 Ω	8000 Ω
R_{el}	4.58×10^7 Ω	4.89×10^7 Ω
C_g	4.58×10^{-12} F	5.40×10^{-11} F
C_{gb}	1.37×10^{-9} F	2.29×10^{-9} F
C_{el}	5.81×10^{-11} F	6.85×10^{-11} F
T_g	8.39×10^{-9} sec	8.83×10^{-8} sec
T_{gb}	4.12×10^{-7} sec	1.83×10^{-5} sec
T_{el}	2.66×10^{-3} sec	3.35×10^{-3} sec

4.58×10^{-12} F. It revealed interfacial capacitance was higher due to space charge accumulation (higher resistivity is due to charge depletion) at grain boundaries due to lower resistance 300 Ω than grain resistance 1830 Ω. After applying magnetic field, grain resistance slightly decreased to 1634 Ω exhibiting increased response of charge carriers (Table I). Grain capacitance has been increased from 4.58×10^{-12} to 5.40×10^{-11} F by the application of magnetic field. It is contrary to the M-W model that lower resistive charge carrier (grain boundary 300 Ω) would respond as magnetic field applied. No significant effect on interfacial grain boundary capacitance has observed due to applied magnetic field. Grain capacitance response is mainly due to electric dipole moment only.[34] It revealed coupling of magnetic dipoles with electric dipoles. Magnetic and electric dipoles individually formed their respective domains inside the grain and around grain boundaries which are supported by M-H loop and P-E loop as shown in Figures 2(a) and 1(b). Magnetoelectric coupling effect due to close interaction between electric and magnetic domains is confirmed by ME coupling coefficient measurement. It may be suggested doped Cr^{3+} ion replacing Ti^{4+} ions and oxygen vacancies have been created for compensating charge. These oxygen vacancies are the exchange bridge among Cr^{3+} ions inducing ferromagnetism. When magnetic field applied the magnetic moment of Cr^{3+} try to align parallel to the field that influences the position of Ti^{4+} ions bonded with oxygen orbitals. Hence, capacitance of the BTO lattice/grain increased. Grain boundary resistance increased highly from 300 Ω to 8000 Ω by applying magnetic field. In this case, increase in grain boundary resistance of Cr:BTO film at high frequency by applied magnetic field may be due to depletion of oxygen vacancies involved in exchange interaction.[35,36] Relaxation time of charge carrier inside grains is increased by magnetic field due to high frequency response of electric dipoles.

Magnetic Cr:BTO ferroelectric thin film has been investigated for magnetoelectric coupling coefficient by dynamic method. Dynamic method is the most reliable ME coefficients measurement among four methods.[37–39] Magnetoelectric coupling coefficient in presence of DC bias magnetic field at fixed frequency f = 249 kHz and magnitude 0.5 Oe has been measured. See supplementary material for Fig. S1.[40] The highest magnetoelectric coupling coefficient has been obtained 137 mV/cm-Oe at 1000 Oe magnetic field. It reveals at 1000 Oe DC magnetic field and 0.5 Oe, 249 kHz AC frequency magnetic field, charge carriers involved in exchange coupling exhibit maximum displacement. Further with increase in DC field, torque on magnetic dipoles disturbing the maximum displacement of charge carriers thus voltage induced exhibits a maximum value which ultimately decreases with increase in applied magnetic field. It has been analyzed by magneto impedance spectroscopy that capacitance of grain increases with applied magnetic field. A significant value 137 mV/cm-Oe of ME coupling coefficient has been observed for single layer magnetoelectric thin film.

Chromium doped induced ferromagnetic Cr:BTO ferroelectric thin film has been investigated for the origin of magnetoelectric coupling. By theoretical impedance equation fitted to experimental data in Cole-Cole plot, contribution of individual grains, grain boundaries, and electrode has been deconvoluted. It has been observed that increase in capacitance is due to BTO lattice response obtained by grains with applied magnetic field from curve fitting. Further, magnetoelectric coupling performed by dynamic method at high frequency has been also confirmed the coupling of charge carrier within lattice. A significant value 137 mV/cm-Oe of magnetoelectric coupling has been obtained in single phase and single layer multiferroic thin film. The high value of ME coupling obtained can reduce the typical processing steps involved in multilayer deposition of different compounds. Barium titanate being best ferroelectric material has been tailored to be multiferroic by non ferromagnetic element, Cr, doping in thin film form opens an avenue for more stable and reliable spintronic material for low power magnetoelectric random excess memory applications.

The authors are grateful to the Director "National Physical Laboratory" New Delhi for providing constant encouragement and support to carry out this work.

[1]C. Binek, Physics **6**, 13 (2013).
[2]G. Lawes and G. Srinivasan, J. Phys. D: Appl. Phys. **44**, 243001 (2011).
[3]M. Li, Y. Wang, Y. Shen, J. Gao, J. Li, and D. Viehland, J. Appl. Phys. **114**, 144501 (2013).
[4]Y. Chen, J. Wang, M. Liu, J. Lou, N. X. Sun, C. Vittoria, and V. G. Harris, Appl. Phys. Lett. **93**, 112502 (2008).
[5]Z. Zhou, T. X. Nan, Y. Gao, X. Yang, S. Beguhn, M. Li, Y. Lu, J. L. Wang, M. Liu, K. Mahalingam, B. M. Howe, G. J. Brown, and N. X. Sun, Appl. Phys. Lett. **103**, 232906 (2013).
[6]R. Jahns, A. Piorra, E. Lage, C. Kirchhof, D. Meyners, J. L. Gugat, M. Krantz, M. Gerken, R. Knochel, and E. Quandt, J. Am. Ceram. Soc. **96**(6), 1673–1681 (2013).
[7]H. Zhao, X. Peng, L. Zhang, J. Chen, W. Yan, and X. Xing, Appl. Phys. Lett. **103**, 082904 (2013).
[8]J. Zhai, Z. Xing, S. Dong, J. Li, and D. Viehland, J. Am. Ceram. Soc. **91**(2), 351–358 (2008).
[9]Y. Lin, N. Cai, J. Zhai, G. Liu, and C.-W. Nan, Phys. Rev. B **72**, 012405 (2005).
[10]N. Jedrecy, H. J. von Bardeleben, V. Badjeck, D. Demaille, D. Stanescu, H. Magnan, and A. Barbier, Phys. Rev. B **88**, 121409(R) (2013).
[11]W. Liang, Z. Li, Z. Bi, T. Nan, H. Du, C. Nan, C. Chen, Q. Jia, and Y. Lin, J. Mater. Chem. C **2**, 708–714 (2014).
[12]S. Mukherjee, A. Roy, S. Auluck, R. Prasad, R. Gupta, and A. Garg, Phys. Rev. Lett. **111**, 087601 (2013).
[13]G. Catalan, Appl. Phys. Lett. **88**, 102902 (2006).
[14]M. G. Masud, B. K. Chaudhuri, and H. D. Yang, J. Phys. D: Appl. Phys. **44**, 255403 (2011).
[15]R. Schmidt, J. Ventura, E. Langenberg, N. M. Nemes, C. Munuera, M. Varela, M. Garcia-Hernandez, C. Leon, and J. Santamaria, Phys. Rev. B **86**, 035113 (2012).
[16]T. Kambe, Y. Fukada, J. Kano, T. Nagata, H. Okazaki, T. Yokoya, S. Wakimoto, K. Kakurai, and N. Ikeda, Phys. Rev. Lett. **110**, 117602 (2013).
[17]J. Shah and R. K. Kotnala, J. Mater. Chem. A **1**, 8601–8608 (2013).
[18]Y.-H. Lin, J. Yuan, S. Zhang, Y. Zhang, J. Liu, Y. Wang, and C.-W. Nan, Appl. Phys. Lett. **95**, 033105 (2009).
[19]E. V. Ramana, S. M. Yang, R. Jung, M. H. Jung, B. W. Lee, and C. U. Jung, J. Appl. Phys. **113**, 187219 (2013).
[20]V. Sharma, G. Pilania, G. A. Rossetti, Jr., K. Slenes, and R. Ramprasad, Phys. Rev. B **87**, 134109 (2013).
[21]I. N. Apostolova, A. T. Apostolov, S. G. Bahoosh, and J. M. Wesselinowa, J. Appl. Phys. **113**, 203904 (2013).
[22]H. Nakayama and H. Katayama-Yoshida, Jpn. J. Appl. Phys., Part 2 **40**, L1355–L1358 (2001).
[23]S. Ray, P. Mahadevan, S. Mandal, S. R. Krishnakumar, C. S. Kuroda, T. Sasaki, T. Taniyama, and M. Itoh, Phys. Rev. B **77**, 104416 (2008).
[24]H. Liu, B. Cao, and C. O'Connor, J. Appl. Phys. **109**, 07B516 (2011).
[25]W. Li, R. Zhao, L. Wang, R. Tang, Y. Zhu, J. H. Lee, H. Cao, T. Cai, H. Guo, C. Wang, L. Ling, L. Pi, K. Jin, Y. Zhang, H. Wang, Y. Wang, S. Ju, and H. Yang, Sci. Rep. **3**, 2618 (2013).
[26]Y. Watanabe, M. Tanamura, S. Matsumoto, and Y. Seki, J. Appl. Phys. **78**(3), 2029 (1995).

[27]J. Lappalainen, J. Frantti, and V. Lantto, J. Am. Ceram. Soc. **82**(4), 889–896 (1999).
[28]K. Chesnel, B. Wilcken, M. Rytting, S. D. Kevan, and E. E. Fullerton, New J. Phys. **15**, 023016 (2013).
[29]N. H. Hong, A. Ruyter, F. Gervais, W. Prellier, and J. Sakai, J. Appl. Phys. **97**, 10D323 (2005).
[30]H. M. Jang, J. H. Park, S. Ryu, and S. R. Shannigrahi, Appl. Phys. Lett. **93**, 252904 (2008).
[31]M. P. Singh, W. Prellier, Ch. Simon, and B. Raveau, Appl. Phys. Lett. **87**, 022505 (2005).
[32]C. W. Nan, X. Zhou, J. Nan, and J. Wu, J. Appl. Phys. **89**, 3955 (2001).
[33]J. C. C. Abrantes, J. A. Labrincha, and J. R. Frade, Mater. Res. Bull. **35**, 727–740 (2000).
[34]D. C. Sinclair, Bol. Soc. Esp. Cerám. Vidrio **34**(2), 55–65 (1995). Available at http://boletines.secv.es/upload/199534055.pdf.
[35]M. Foygel, J. Niggemann and A. G. Petukhov, IEEE Trans. Magn. **43**, 3040 (2007).
[36]M. T. Buscaglia, V. Buscaglia, M. Viviani, and P. Nanni, J. Am. Ceram. Soc. **84**(2), 376–384 (2001).
[37]K. H. J. Buschow, *Handbook of Magnetic Materials* (Elsevier-Science, 2012), Vol. 20, pp. 161–164.
[38]J. P. Rivera, Eur. Phys. J. B **71**, 299–313 (2009).
[39]G. V. Duong, R. Groessinger, M. Schoenhart, and D. Bueno-Basques, J. Magn. Mater. **316**, 390–393 (2007).
[40]See supplementary material at http://dx.doi.org/10.1063/1.4870263 for Fig. S1.